

## Detection of Acoustic Pulses in River Sand: Experiment

V. Yu. Zaitsev\*, A. B. Kolpakov\*\*, and V. E. Nazarov\*

\* Institute of Applied Physics, Russian Academy of Sciences, ul. Ul'yanova 46, Nizhni Novgorod, 603600 Russia

\*\* Nizhni Novgorod State Architecture–Construction University, ul. Il'inskaya 65, Nizhni Novgorod, 603600 Russia

Received March 25, 1998

**Abstract**—Experimental results on the parametric generation and propagation of low-frequency video-pulse signals formed as a result of the detection of high-frequency acoustic pulses in dry and water-saturated river sand are presented. The dependence of the propagation velocity of video pulses on the static pressure, the dependence of the video-pulse amplitude on the amplitude of the pumping wave, and the relation between the shape of the detected pulse and the envelope of the pumping pulse under different static loading of the medium are studied experimentally. Nonlinear equations of state adequately describing the observed phenomena in dry and water-saturated sand are obtained on the basis of the analysis of the experimental results.

### INTRODUCTION

The linear propagation of elastic waves in granular media (for example, in river sand) has been extensively studied [1–5]. It was found that low propagation velocities and extremely high attenuation of elastic waves are typical of these media. As a result, an opinion was formed that “all efforts in transmitting high-frequency signals through loose granular media similar to unloaded sand are doomed to fail” [2].

From the viewpoint of nonlinear acoustics, granular media are of particular interest, because they exhibit high nonlinear properties, which provide strong interaction between elastic waves of even relatively low amplitudes. When a high-frequency amplitude-modulated acoustic wave travels in a nonlinear medium, it is detected; as a result, a secondary low-frequency wave is generated in the medium. This wave decays slowly even in sand, and it can be used for sounding the medium. (Note that parametric acoustic radiators successfully used in hydroacoustics [6] are based on this principle.) On the other hand, idealized models and equations of state describing granular media were developed in recent years [5, 7–10]. In this regard, the results of experimental studies of nonlinear acoustic effects in granular media can be employed for refining these models and the equations of state. In addition, many rocks can be treated as granular media. Therefore, these studies are also of interest from the viewpoint of possible diagnostic applications (in seismic engineering, seismic prospecting, etc.).

In this paper, we present the results of an experimental study of acoustic pulse detection and propagation in dry and water-saturated river sand. On the basis of the analysis of the experimental dependences, we determine the equations of state for these media.

### DESCRIPTION OF THE EXPERIMENT

A block-diagram of the experimental setup is shown in Fig. 1. A 20-cm-high glass pipe (2) with a diameter of 19 cm containing dry or water-saturated sand (3) is mounted on a platform (1). The average size of the grains of sand is about  $2 \times 10^{-2}$  cm and the sand porosity is about 43%. The water-saturated medium is modeled by placing the sand into water. The high-frequency acoustic pulses are generated in sand with the help of a radiator (a longitudinal vibrator) (4) buried in sand 10 cm below its surface. The vibrator diameter is 8 cm; the pulse carrier frequency is 180 kHz. A system of weights (5) of the total mass  $M \leq 26$  kg is used to create the static pressure  $P_0$  in sand. The weights are placed on a 4-mm-thick acrylic plastic plate (6) of mass  $m = 120$  g. The plate completely covers the pipe cross-section so

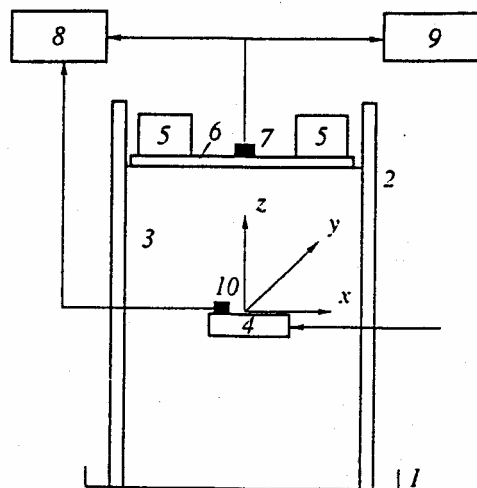


Fig. 1. Block-diagram of the experiment: (1) platform; (2) glass pipe; (3) river sand; (4) radiator; (5) system of weights; (6) plate; (7) accelerometer; (8) two-channel digital oscilloscope; (9) spectrum analyzer; and (10) control accelerometer.

that the static pressure can be calculated as  $P_0 = (M + m)g/S$ , where  $g$  is the free fall acceleration and  $S$  is the pipe cross-section. An accelerometer (7) responding to the vertical component of the plate acceleration  $A = A(t)$  is glued to the plate (6) at its center coaxially with the radiator in order to record the detected signal. The signal from the accelerometer is supplied to the first input of a digital oscilloscope (8) and to the input of a spectrum analyzer (9). The radiated signal is monitored by an accelerometer (10) glued to the radiator, and the signal from this accelerometer is supplied to the second input of the oscilloscope.

Two modes of the high-frequency pulse radiation are used in the experiment: the single-pulse mode (short pulses of duration  $70 \mu\text{s}$  and long pulses of duration  $1300 \mu\text{s}$ ) and the mode of radiating a train of short pulses at a pulse repetition frequency  $F = 3150 \text{ Hz}$ .

EXPERIMENTAL RESULTS

When single (short or long) high-frequency acoustic pulses are excited in a nonlinear medium such as sand, they become detected. Oscillograms of the radiated and detected signals are plotted in Figs. 2 and 3. The comparison between the high-frequency and low-frequency pulses shows that the shape of a detected pulse is close to the third time derivative of the pumping pulse envelope. The measurements show that the duration of the detected pulses noticeably decreases with an increase in the static pressure  $P_0$ , because attenuation of the elastic waves in sand decreases with an increase in  $P_0$  [2, 5]. Figure 4 plots the characteristic duration  $T^*$  of the video signals (see notation in Fig. 2) as a function of the static pressure  $P_0$  for the short high-frequency pulses excited in dry and water-saturated sand.

As the static pressure  $P_0$  increases, a decrease  $\Delta T$  in the propagation time (i.e., an increase in the propagation velocity) and an increase in the amplitude of the detected pulses are observed. The latter result testifies to the fact that an increase in the static pressure  $P_0$  reduces the attenuation of elastic waves in sand to a greater extent than it reduces the elastic nonlinearity of sand.

Figure 5 plots (on the logarithmic scale) the average velocity  $\bar{c}(P_0) = L/\Delta T(P_0)$  (where  $L$  is the distance between the radiator and the accelerometer) of the video pulses propagating in dry and water-saturated sand as a function of the static pressure  $P_0$ . These dependences also show that, for the loads  $P_0 \geq 2 \times 10^3 \text{ Pa}$  (when the pressure in the medium is dominated by the system of weights with the total mass  $M \geq 5.6 \text{ kg}$ ), the function  $\bar{c} = \bar{c}(P_0)$  has the form

$$\bar{c}(P_0) \sim P_0^m, \tag{1}$$

where  $m = 1/6$ . (Similar exponential dependences of the elastic wave velocity on pressure were observed in [1, 2].)

Note that function (1) with the exponent  $m = 1/6$  corresponds to the equation of state of a granular

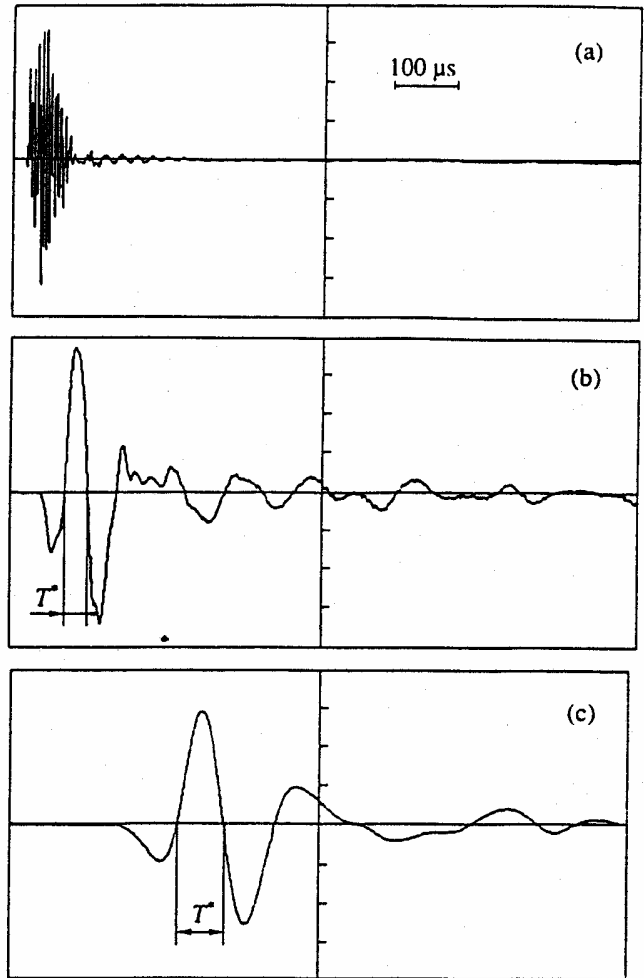


Fig. 2. Oscillograms of (a) a short pumping pulse and the detected video pulses in (b) dry and (c) water-saturated sand under the static pressure  $P_0 = 3.9 \times 10^3 \text{ Pa}$ .

medium [1, 9] consisting of identical perfectly elastic balls interacting in compliance with the Hertz law:

$$\sigma = -B(-\epsilon)^{3/2}, \tag{2}$$

where  $B = \bar{n}(1 - \Delta)E/3\pi(1 - \nu^2)$ ,  $\sigma$  and  $\epsilon$  are the longitudinal compression stress and strain;  $\bar{n}$  is the average number of contacts per particle of the medium;  $E$  and  $\nu$  are, respectively, Young's modulus and Poisson's ratio of the solid phase of the medium; and  $\Delta$  is the porosity of the granular medium.

Figure 6 plots the amplitude  $A_0$  of the video signals produced by single short high-frequency pulses excited in the dry and water-saturated sand as a function of the static pressure  $P_0$ . This figure reveals that, for  $P_0 \geq 2 \times 10^3 \text{ Pa}$ ,

$$A_0 \sim P_0^d, \tag{3}$$

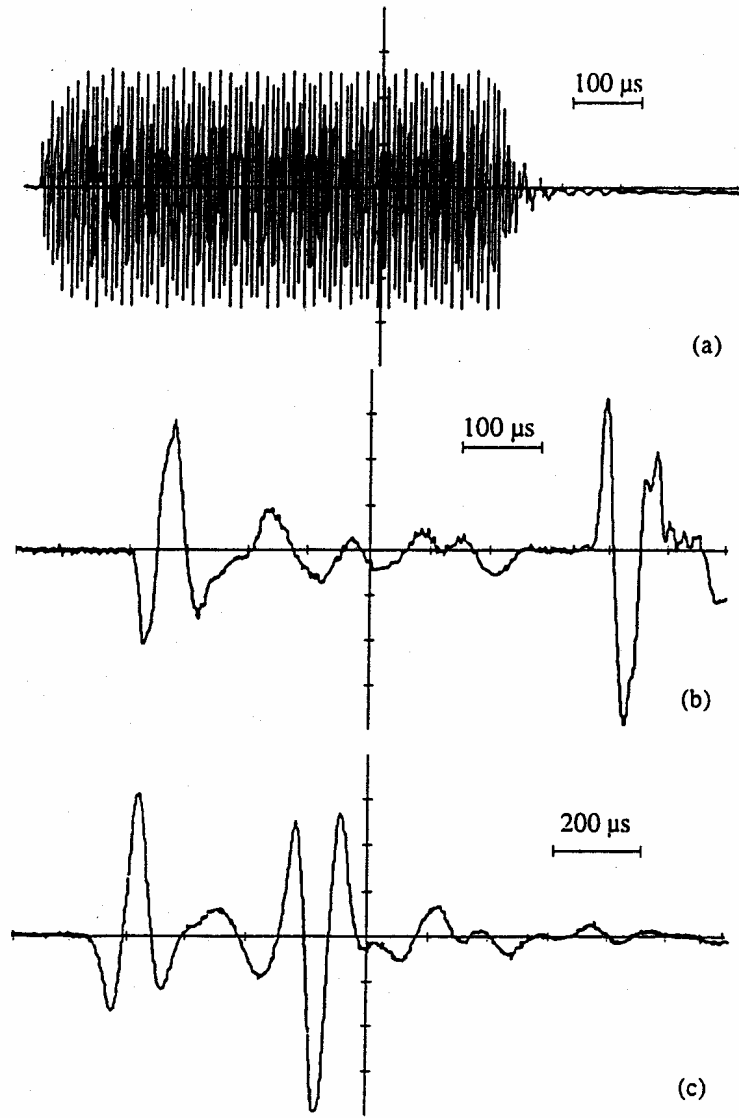


Fig. 3. Oscillograms of (a) a long pumping pulse and the detected video pulses in (b) dry and (c) water-saturated sand under the static pressure  $P_0 = 9 \times 10^3$  Pa.

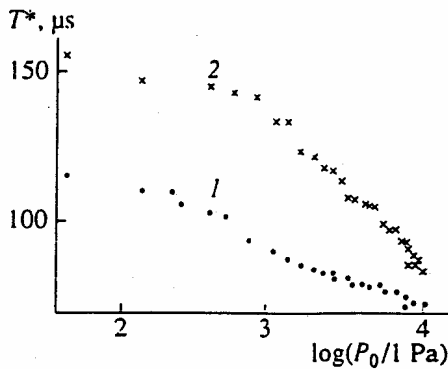


Fig. 4. Characteristic duration  $T^*$  of the video pulses produced in (1) dry and (2) water-saturated sand by short high-frequency pulses versus the static pressure  $P_0$ .

where  $d \approx 1/3$  and  $1/2$  for dry and water-saturated sand, respectively.

We also measured the amplitudes  $A_0$  of the detected pulses as a function of the strain amplitude  $\mathcal{E}$  of the short pumping pulses produced by the radiator. These functions for different static pressures  $P_0$  are displayed in Fig. 7 for (1) dry and (2) water-saturated sand. The figure shows that

$$A_0 \sim \mathcal{E}^n, \tag{4}$$

where  $n \approx 3/2$ .

In the mode of generating a train of equispaced short signals, the accelerometer (7) received continuous low-frequency detected signals, whose spectra are shown in Figs. 8a and 8b for dry and water-saturated sand,

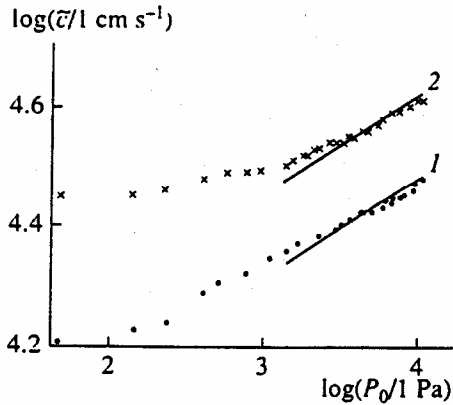


Fig. 5. Average video pulse velocity in (1) dry and (2) water-saturated sand versus the static pressure. The straight lines correspond to the function  $\bar{c}(P_0) \sim P_0^{1/6}$ .

respectively. The spectra of these signals are fairly complex and contain the pulse repetition frequency  $F$  and its higher harmonics  $pF$ ,  $p = 1, 2, \dots$ . Figures 9a and 9b show the amplitudes  $A(pF)$  of the first three harmonics of the repetition frequency  $F$  in the spectra of the detected signals versus the strain amplitude  $\epsilon_0$  of the pumping pulse for dry and water-saturated sand, respectively. These figures show that, for dry and water-saturated sand,  $A(pF) \sim \epsilon_0^n$ , where  $n = 3/2$ . As expected, this result complies with dependence (4) obtained above for the case of single short pulses.

Below, relationships (1), (3), and (4) determined from the experiments will be used to derive the equations of state adequately describing the operation of a parametric acoustic radiator in dry and water-saturated sand.

EQUATION OF STATE FOR DRY SAND

In the experiments with dry sand, relationships (1) and (4), which describe the wave propagation velocity as a function of the static pressure and the amplitude of the detected pulse as a function of the pumping pulse amplitude, were established. In order to explain dependence (1), one can assume that the equation of state has the form of equation (2), in which, however, the stress  $\sigma$  and strain  $\epsilon$  should be replaced, respectively, by  $-P_0 + \sigma$  and  $\epsilon_0 + \epsilon$  ( $|\sigma| < P_0$  and  $|\epsilon| < |\epsilon_0|$ ), where  $\epsilon_0$  is the static strain of the medium determined by the static pressure  $P_0$  as

$$P_0 = B(-\epsilon_0)^{3/2}, \tag{5}$$

and  $\sigma$  and  $\epsilon$  are, respectively, the stress and strain in the elastic wave.

With allowance for the results obtained above, equation (2) cannot be used to explain relationship (4), because it predicts a quadratic dependence of  $A_0$  on  $\epsilon$

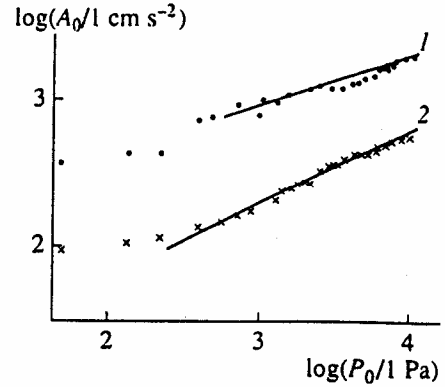


Fig. 6. Amplitude  $A_0$  of the video signals versus the static pressure  $P_0$  for (1) dry and (2) water-saturated sand in the case of the generation of short high-frequency pulses. The straight lines correspond to the functions (1)  $A_0 \sim P_0^{1/3}$  and (2)  $A_0 \sim P_0^{1/2}$ .

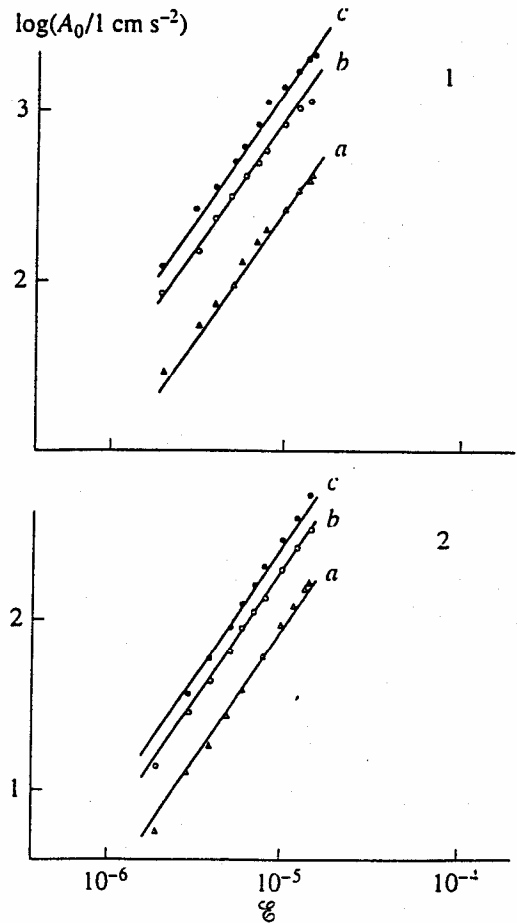


Fig. 7. Amplitude  $A_0$  of the video signals versus the strain amplitude  $\epsilon$  of the short pumping pulses for (1) dry and (2) water-saturated sand for different static pressures:  $P_0 = (a) 5.7 \times 10^2$ ,  $(b) 3.9 \times 10^3$ , and  $(c) 9 \times 10^3$  Pa. The straight lines correspond to the function  $A_0 \sim \epsilon^{3/2}$ .

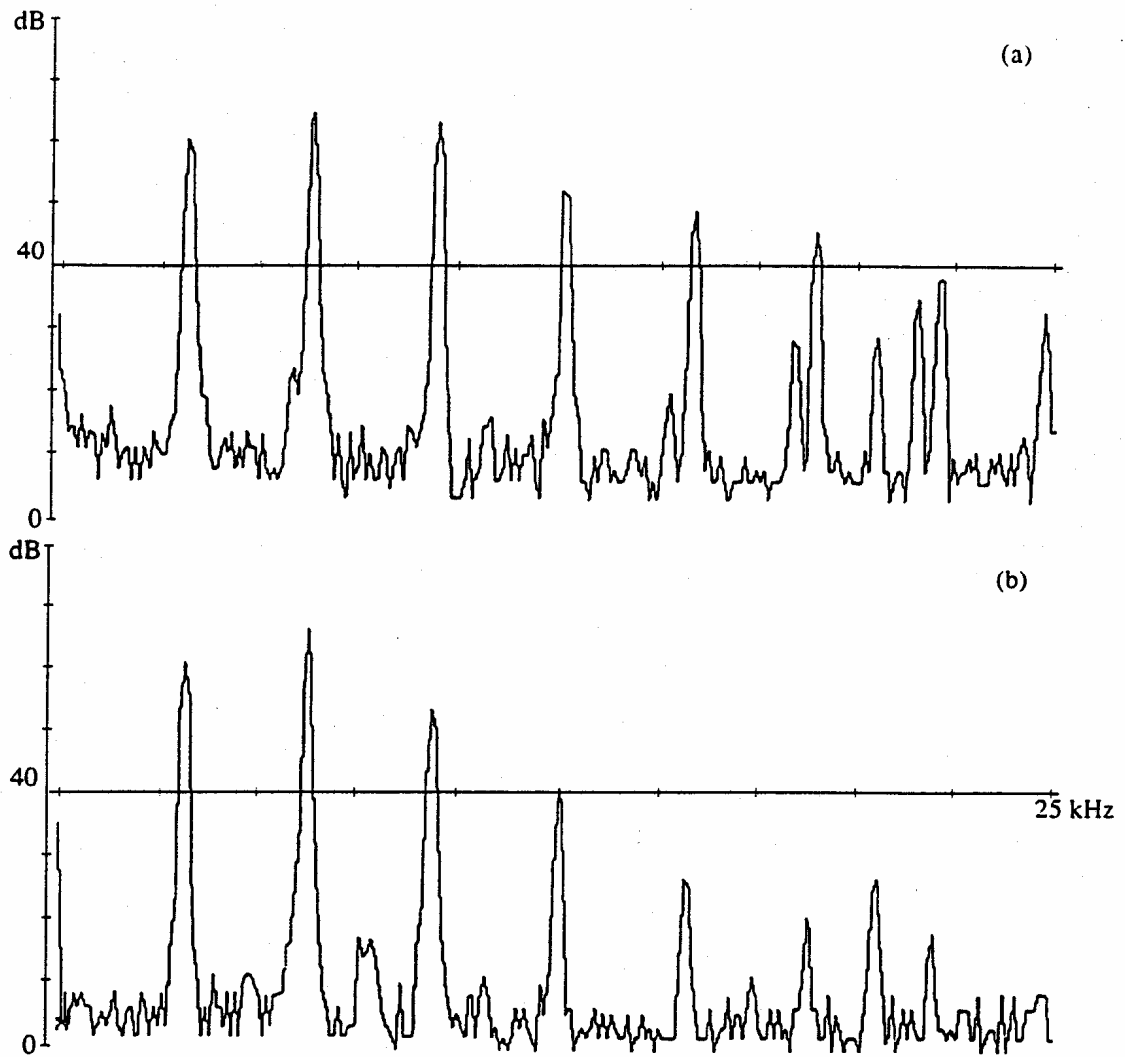


Fig. 8. Spectra of the detected signals for (a) dry and (b) water-saturated sand.

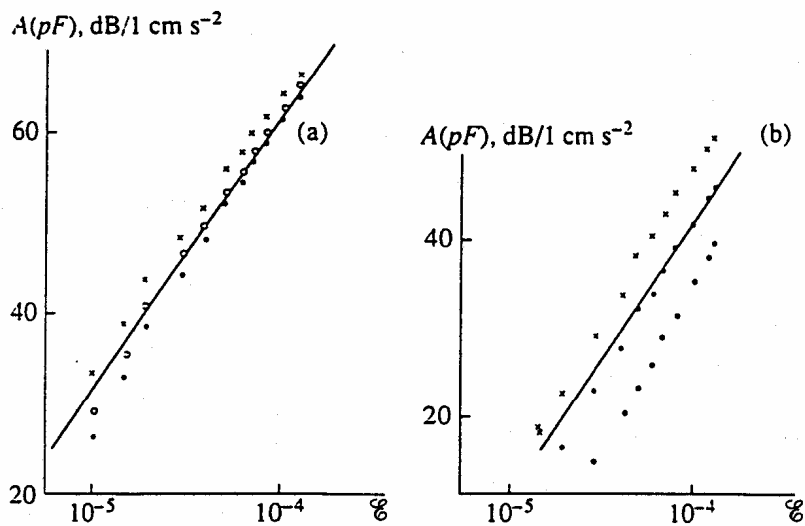


Fig. 9. Amplitudes of the first three harmonics of the pulse repetition frequency in the spectrum of the detected signals versus the strain amplitude of the pumping pulses for (a) dry and (b) water-saturated sand:  $p = (\bullet) 1, (\times) 2, \text{ and } (\circ) 3$ . The straight lines correspond to the function  $A(pF) \sim \varepsilon^{3/2}$ ;  $P_0 = 9 \times 10^3 \text{ Pa}$ .

for  $|\epsilon| \ll |\epsilon_0|$ . Besides, equation of state (2) is valid for a granular medium consisting of identical balls. Actually, river sand consists of grains of various shapes and sizes [1], and some grains can be packed loosely being in an incomplete contact with surrounding tightly packed grains. Mathematically, this situation leads to the introduction of an additional small term describing the so-called flapping nonlinearity of the Hertzian type due to loosely packed grains [11, 12]. As indicated in [12], in the simplest case, this nonlinearity can be adequately described by a constant small compression  $g\epsilon_0$ , where  $|g| \ll 1$ . As a result, the equation of state for dry sand takes the form

$$\sigma - P_0 = -B(-\epsilon - \epsilon_0)^{3/2} - \alpha(-\epsilon - g\epsilon_0)^{3/2} h(-\epsilon - g\epsilon_0),$$

where  $\alpha = \alpha(P_0)$  and  $h(\cdot)$  is the Heaviside function.

For small acoustic perturbation, when  $|\epsilon/\epsilon_0| \ll (8\alpha/3B)^2 \epsilon_0^2$  and  $|\epsilon/\epsilon_0| \ll 1$ , equations (4) and (5) yield

$$\begin{aligned} \sigma(\epsilon) = & (3b/2)(-\epsilon_0)^{1/2} \epsilon \\ & + \alpha(-\epsilon - g\epsilon_0)^{3/2} h(-\epsilon - g\epsilon_0). \end{aligned} \quad (6)$$

It can be easily seen that equation (6) describes relationships (1) and (4) established in the experiment: the first summand determines the velocity of the video pulse  $\bar{c}(P_0) = (3/2\rho)^{1/2} (B^2 P_0)^{1/6}$  (where  $\rho$  is the density of the medium), while the second one (for  $|\epsilon| \gg |g\epsilon_0|$ ) describes the video pulse amplitude  $A_0$  as a function of the pumping pulse amplitude  $\mathcal{E}$ .

#### EQUATION OF STATE FOR WATER-SATURATED SAND

The experiments with water-saturated sand showed that, qualitatively, the dependences of the propagation velocity of the detected pulse on the static pressure and the dependences of the detected pulse amplitude on the amplitude of the pumping pulse are similar to those observed for dry sand. As seen from Fig. 7, one of the basic quantitative differences is that, at small static pressures, the average velocity of the detected pulse in water-saturated sand is higher than the velocity in dry sand. This fact testifies that, in the presence of water, sand exhibits a linear elastic modulus already at a zero static pressure, which is not observed in dry sand. Therefore, in order to describe water-saturated sand, the equation of state for dry sand should be complemented with a linear term  $D\epsilon$ :

$$\begin{aligned} \sigma(\epsilon) = & (D + (3b/2)(-\epsilon_0)^{1/2}) \epsilon \\ & + \alpha(-\epsilon - g\epsilon_0)^{3/2} h(-\epsilon - g\epsilon_0), \end{aligned} \quad (7)$$

where  $D$  is the linear elastic modulus that appears in water-saturated sand due to the presence of water.

Equation (7) yields an expression for the sound velocity

$$c = c_0(1 + (3b/2D)(P_0/B)^{1/3})^{1/2},$$

where  $c_0 = (D/\rho)^{1/2}$ .

At low static pressure, we have  $c \approx c_0 \approx \text{const}$ , while, at high pressure,  $c(P_0) \sim P_0^{1/6}$ , as for dry sand.

Subsequently, we will describe the detection of acoustic pulses under the assumption that  $g = 0$ .

#### CONCLUSION

This paper experimentally studies the processes of the parametric generation of low-frequency video-pulse signals formed as a result of detection of high-frequency acoustic pulses in dry and water-saturated sand. The dependence of the velocity of a detected pulse on the static pressure, the dependence of the video-pulse amplitude on the amplitude of the pumping pulse, and the relationship between the shape of the detected pulse and the envelope of the pumping pulse are determined.

The specific feature of the experiments is that they are complex: they include the measurements of both elastic and inelastic (dissipative) linear characteristics of the medium, and the nonlinear properties of the medium are studied on the basis of various static and wave effects.

Our next paper will present a detailed theoretical description of the operation of a parametric acoustic radiator in river sand on the basis of the equations of state (6) and (7) established above.

#### ACKNOWLEDGMENTS

This work was supported by the Russian Foundation for Basic Research, project nos. 98-02-17686 and 98-05-64683.

#### REFERENCES

1. Tsareva, N.V., Elastic Wave Propagation in Sand, *Izv. Akad. Nauk SSSR, Ser. Geofiz.*, 1956, no. 1, pp. 1044-1053.
2. Antsiferov, M.S., Antsiferova, N.G., and Kagan, Ya. Ya., Ultrasonic Wave Propagation in Sand under Pressure, *Izv. Akad. Nauk SSSR, Ser. Geofiz.*, 1964, no. 12, pp. 1774-1781.
3. Parkhomenko, I.S., On the Frequency Dependence of Elastic Wave Attenuation in Sand, *Fiz. Zemli*, 1967, no. 8, pp. 101-109.
4. Buckingham, M.J., Theory of Acoustic Attenuation, Dispersion, and Pulse Propagation in Unconsolidated Granular Material Including Marine Sediments, *J. Acoust. Soc. Am.*, 1997, vol. 102, no. 5, part 1, pp. 2579-2596.
5. White, J.E., *Underground Sound: Application of Seismic Waves*, Amsterdam: Elsevier, 1983.

6. Novikov, B.K., Rudenko, O.V., and Timoshenko, V.I., *Nelineinaya gidroakustika* (Nonlinear Underwater Acoustics), Leningrad, 1981.
7. Nesterenko, V.F., Propagation of Nonlinear Pressure Pulses in Granular Media, *Zh. Prikl. Mekh. Tekh. Fiz.*, 1983, no. 5, pp. 136–148.
8. Lazaridi, A.N. and Nesterenko, V.F., Detection of a New Type of Solitary Waves in a One-Dimensional Granular Medium, *Zh. Prikl. Mekh. Tekh. Fiz.*, 1985, no. 3, pp. 115–118.
9. Belyaeva, I.Yu., Zaitsev, V.Yu., and Ostrovskii, L.A., Nonlinear Acoustoelastic Properties of Granular Media, *Akust. Zh.*, 1993, vol. 39, no. 1, pp. 25–32 [*Acoust. Phys.*, vol. 39, no. 1, pp. 11–14].
10. Bogdanov, A.N. and Skvortsov, A.G., Nonlinear Shear Waves in a Granular Medium, *Akust. Zh.*, 1992, vol. 38, no. 3, pp. 408–412 [*Sov. Phys. Acoust.*, vol. 38, no. 3, pp. 224–225].
11. Belyaeva, I.Yu., Zaitsev, V.Yu., and Timanin, E.M., Experimental Study of Nonlinear Elastic Properties of Granular Media with Nonideal Packing, *Akust. Zh.*, 1994, vol. 40, no. 6, pp. 893–898 [*Acoust. Phys.*, vol. 40, no. 6, pp. 789–793].
12. Zaitsev, V.Yu., Nonideally Packed Granular Media: Numerical Modeling of Elastic Nonlinear Properties, *Akust. Zh.*, 1995, vol. 41, no. 3, pp. 439–445 [*Acoust. Phys.*, vol. 41, no. 3, pp. 385–391].

*Translated by A.D. Khzmalyan*